Cyclosporin-A-induced prion protein aggresomes are dynamic quality-control cellular compartments

Tziona Ben-Gedalya[1], Roman Lyakhovetsky[2], Yifat Yedidia[1,*], Michal Bejerano-Sagie[1], Natalya M. Kogan[3], Marcela Viviana Karpuj[4], Daniel Kaganovich[2] and Ehud Cohen[1,‡]

[1]Biochemistry and Molecular Biology, Institute for Medical Research Israel-Canada (IMRIC), Hebrew University Medical School, Jerusalem 91120, Israel
[2]Department of Cell and Developmental Biology, Alexander Silberman Institute of Life Sciences, Hebrew University of Jerusalem, Givat-Ram, Jerusalem 91904, Israel
[3]Medicinal Chemistry and Natural Products Department, Pharmacy School, Hebrew University Medical School, Jerusalem 91120, Israel
[4]Institute of Biochemistry, Food Science and Nutrition, Food and Environmental Quality Sciences, Faculty of Agriculture, Hebrew University of Jerusalem, Rehovot 76100, Israel

*Present address: The Infectious Diseases Unit, Shaare Zedek Medical Center, Jerusalem 91031, Israel, affiliated with the Hadassah-Hebrew University Medical School
‡Author for correspondence (ehudc@ekmd.huji.ac.il)

Accepted 23 January 2011
Journal of Cell Science 124, 1891-1902

doi:10.1242/jcs.077693

Summary

Despite the activity of cellular quality-control mechanisms, subsets of mature and newly synthesized polypeptides fail to fold properly and form insoluble aggregates. In some cases, protein aggregation leads to the development of human neurodegenerative maladies, including Alzheimer's and prion diseases. Aggregates of misfolded prion protein (PrP), which appear in cells after exposure to the drug cyclosporin A (CsA), and disease-linked PrP mutants have been found to accumulate in juxtanuclear deposition sites termed 'aggresomes'. Recently, it was shown that cells can contain at least two types of deposition sites for misfolded proteins: a dynamic quality-control compartment, which was termed 'JUNQ', and a site for terminally aggregated proteins called 'IPOD'. Here, we show that CsA-induced PrP aggresomes are dynamic structures that form despite intact proteasome activity, recruit chaperones and dynamically exchange PrP molecules with the cytosol. These findings define the CsA–PrP aggresome as a JUNQ-like dynamic quality-control compartment that mediates the refolding or degradation of misfolded proteins. Together, our data suggest that the formation of PrP aggresomes protects cells from proteotoxic stress.

Key words: Aggregation, Aggresome, Cyclosporin A, Prion protein, Proteasome

Introduction

Specialized chaperones assist nascent polypeptides to attain their functional, native structure and ensure their folding integrity (Hartl and Hayer-Hartl, 2009). Despite these cellular folding and quality-control mechanisms, subsets of the newly synthesized polypeptides fail to fold properly and are targeted for degradation by the ubiquitin proteasome system (UPS) (Hirsch et al., 2009). Occasionally, aggregation-prone, aberrantly folded proteins escape degradation and form aggregates. In some cases, this process leads to the development of diseases, collectively termed 'conformational disorders' (Kopito and Ron, 2000), including the subgroup of late-onset human neurodegenerative disorders such as Alzheimer's (AD), Parkinson's (PD) (Selkoe, 2003), Huntington's (HD) (Bates, 2003) and prion (Aguzzi and Calella, 2009) diseases.

Cells have developed protective mechanisms that detoxify potentially hazardous protein aggregates through various activities, including disaggregation, degradation and protective active aggregation (Behrends et al., 2006; Cohen et al., 2006; Shorter and Lindquist, 2004). When cellular detoxification mechanisms are overloaded, protein aggregates are transported to and confined in specialized deposition sites in an effort to prevent cellular damage (Bagola and Sommer, 2008). In particular, when proteasomes are inhibited, aggregates are transported along microtubules (Kawaguchi et al., 2003), deposited in the microtubule-organizing center (MTOC) and confined by collapsed vimentin fibers. These cytosolic aggregate deposits were termed 'aggresomes' (Johnston et al., 1998). The discovery of aggresomes raised several key questions. Is UPS impairment a prerequisite for the formation of aggresomes? Do aggresomes play protective roles by sequestering potentially toxic aggregates from the cytosol and are there additional types of aggregate deposition sites?

Recently, our understanding of cellular aggregate deposition sites has been expanded by the discovery that cells sort protein aggregates with different properties into at least two distinct types of deposition sites that can concurrently exist within a single cell (Kaganovich et al., 2008). One site is located in close proximity to the nucleus and functions as a quality-control center that attracts chaperones and proteasomes in order to either refold or degrade misfolded aggregated proteins. This type of deposition site, which contains ubiquitylated misfolded proteins, was termed 'juxta nuclear quality control compartment' (JUNQ) and is a dynamic structure that rapidly exchanges proteins with the cytosol. The other aggregate deposition site, which was termed 'insoluble protein deposit' (IPOD), exhibits different properties. Proteins within the IPOD are immobile and no ubiquitin signal can be detected within these structures. The IPOD did not exchange proteins with the cytosol and did not attract proteasomes (Kaganovich et al., 2008). Because a variety of insoluble protein aggregates were sorted into the IPOD, it appears that this site accumulates terminally aggregated proteins in an effort to sequester them and protect the cell from their toxic effects. Interestingly, in this study, disease-linked amyloidogenic proteins

Journal of Cell Science

were found to accumulate primarily within the IPOD and not in JUNQ (Kaganovich et al., 2008).

The misfolding and aggregation of the prion protein (PrP) is tightly linked to the development of prion diseases. Prion disorders manifest either sporadically, as infectious diseases, or as mutation-linked familial maladies. Whereas the emergence of infectious prion diseases is caused by toxic PrP conformers (PrP^{Sc}) that mediate the conversion of correctly folded PrP (PrP^{C}) molecules into the infectious form, familial prion diseases exhibit more diverged mechanisms of manifestation and clinical dynamics (reviewed in Aguzzi and Calella, 2009). Gerstmann-Sträussler-Scheinker syndrome (GSS) is a late-onset familial prion disorder that stems from the substitution of a proline at either residue P102 (Hsiao et al., 1989) or P105 (Yamazaki et al., 1999) in the sequence of PrP. Although the mechanism underlying GSS is poorly understood, we previously reported that these proline substitutions prevent PrP from folding properly, probably due to the abolishment of a chaperone-recognition site, leading to the misfolding and aggregation of PrP (Cohen and Taraboulos, 2003). The chaperones required for proper PrP folding were found to be cyclophilins, members of the immunophilin group [also termed peptidyl-prolyl *cis*/*trans* isomerases (PPIases)]. Cyclophilins accelerate the isomerization of X-Pro bonds and convert their target polypeptides from a *cis* to a *trans* position using proline as an axis for this turn (Schonbrunner et al., 1991). Cyclophilins are found throughout the cell, including the cytosol and the ER, and are specifically inhibited by the drug cyclosporin A (CsA) (Barik, 2006).

Using CsA to inhibit cyclophilins, we discovered that this treatment induces the formation of aggresomes containing misfolded aggregated PrP in approximately 10% of the cells (Cohen and Taraboulos, 2003). Despite their possible mechanistic links to the development of GSS, the properties of CsA–PrP aggresomes and their relation to the newly defined IPOD and JUNQ deposition sites have not yet been investigated.

Here, we show that CsA treatment induces the formation of PrP aggresomes despite intact proteasome activity. We demonstrate that PrP aggresomes recruit the cellular chaperones heat shock protein (Hsp) 70 and αB-crystallin, but not Hsp40 and Hsp90. Using live-cell imaging of PrP fused to the yellow fluorescent protein (YFP–PrP), we discovered that PrP molecules within the aggresome are mobile, exchanged rapidly with the cytosol and are substrates for proteasomal degradation. Our data also indicate that at least two PrP subpopulations, which exhibit distinct properties, reside within CsA–PrP aggresomes. Finally, we show that PrP aggresomes and IPOD compartments display different properties. These data characterize the CsA–PrP aggresome as a JUNQ-like dynamic protein quality-control compartment and suggest that aggresome formation protects the cell from the hazardous potential associated with misfolded PrP.

Results

CsA–PrP aggresomes attract cellular folding chaperones

The recruitment of molecular chaperones is one of the prominent differences between the JUNQ quality control compartment and the terminal IPOD inclusion. Hsp70 is a key player in protein disaggregation and refolding (Liberek et al., 2008), and is thought to be involved in the suppression of neurodegeneration-linked aggregation (Muchowski and Wacker, 2005). For instance, Hsp70 is recruited to HD-linked polyglutamine (polyQ) aggregates (Kim et al., 2002) and its overexpression suppresses neuropathology in spinocerebellar ataxia type 1 (SCA1) model mice (Cummings et al., 2001). To test whether Hsp70 is recruited to CsA–PrP aggresomes, we used neuroblastoma N_2a cells that stably express moderate levels of the MHM_2 PrP chimera (N_2a-M) (supplementary material Fig. S4D) (Scott et al., 1992). The cells were treated with 30 μg/ml CsA, subjected to dual label immunofluorescence assay using antibodies against either PrP (Fig. 1A, panels III and IV, green channel) or the inducible Hsp70 (Fig. 1A, panels V and VI,

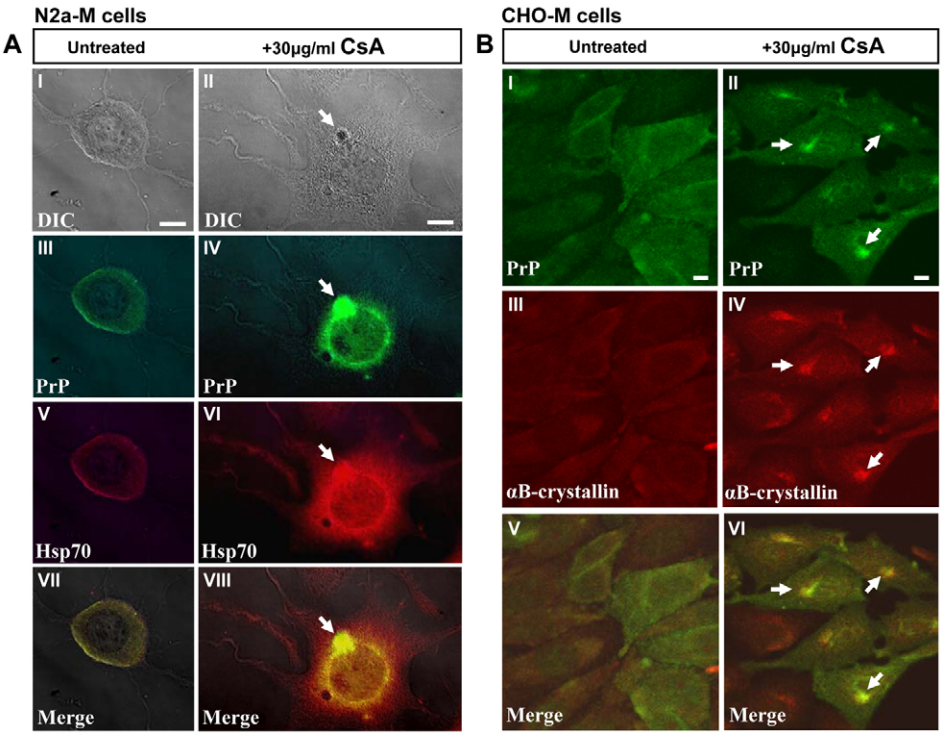

Fig. 1. The heat shock proteins Hsp70 and αB-crystallin are recruited to CsA–PrP aggresomes. (**A**) N2a-M cells were either left untreated (left panels) or incubated with 30 μg/ml CsA (right panels), subjected to immunofluorescence using PrP (panels III and IV) and Hsp70 (panels V and VI) antibodies, and visualized using confocal microscopy. Hsp70 is largely induced in the treated cells and colocalizes with CsA–PrP aggresomes (panel VIII, arrow). (**B**) CHO-M cells were treated as in A and subjected to immunofluorescence using PrP (panels I and II) and αB-crystallin (panels III and VI) antibodies. Visualization using confocal microscopy revealed that αB-crystallin was recruited to PrP aggresomes (panel VI, arrows). Scale bars: 1 μm.

red channel), and visualized using confocal microscopy. Our results indicate that Hsp70 is largely induced and colocalized with CsA–PrP aggresomes of N_2a-M cells (Fig. 1A, panel VIII, arrow). Similar results were observed in CsA-treated CHO cells stably expressing the MHM_2 PrP chimera (CHO-M cells) (supplementary material Fig. S1, arrows). This finding is consistent with the report that constitutively expressed Hsp70 (Hsc70) is recruited to PrP^{Sc}-containing aggresomes (Kristiansen et al., 2005) and suggests a general role for this chaperone in the cellular effort to detoxify toxic PrP conformers.

The small heat shock protein αB-crystallin is also known to suppress the toxicity associated with disease-linked protein aggregation in cell culture (Outeiro et al., 2006) and mice (Muchowski et al., 2008). To test whether this chaperone is recruited to CsA–PrP aggresomes, we employed CsA-treated CHO-M cells and an immunofluorescence assay (as described above) and found that, in a similar manner to Hsp70, αB-crystallin is induced and colocalized with CsA–PrP aggresomes (Fig. 1B). The induction and recruitment of these chaperones to the CsA–PrP aggresomes further suggest that these structures serve as quality-control compartments.

Interestingly, although Hsp40 was reported to suppress polyQ aggregation in concert with Hsp70 (Muchowski et al., 2000) and Hsp90 is known to modulate the aggregation of the PD-linked protein α-synuclein (Falsone et al., 2009), neither Hsp40 nor Hsp90 colocalized with CsA–PrP aggresomes (supplementary material Fig. S2).

The finding that Hsp70 is recruited to CsA–PrP aggresomes enabled us to use this chaperone as a marker and address the question of whether PrP overexpression within a CsA-treated cell is a prerequisite for the formation of an aggresome. We treated naïve CHO cells (which exclusively express the endogenous PrP gene) with CsA and subjected them to immunofluorescence using γ-tubulin and Hsp70 antibodies. CsA treatment has led to the accumulation of Hsp70 in the vicinity of the MTOC (supplementary material Fig. S3), suggesting that PrP overexpression is not required for the formation of these protein quality-control centers within CsA-treated cells.

Intact proteasome activity in the presence of CsA–PrP aggresomes

The clearance of disease-linked toxic protein aggregates is thought to be mediated by the UPS (Ciechanover and Brundin, 2003). Previously, we reported that proteasomes accumulate around CsA–PrP aggresomes, although no ubiquitin conjugates could be detected in these structures (Cohen and Taraboulos, 2003). A similar phenomenon of proteasome accumulation with no detectable ubiquitylation was observed in GFP–250 aggresomes (Garcia-Mata et al., 1999). This apparent contradiction could be explained by rapid UPS-mediated clearance of ubiquitylated PrP molecules, which would prevent their accumulation in the aggresomes. This model predicts intact proteasome activity in CsA-treated aggresome-containing cells. To test this hypothesis, we first measured the rate of UPS activity in the CsA-treated cell culture by adopting two independent proteasomal activity assays: an in vitro assay based on the release of the fluorogenic agent AMC from the synthetic proteasome substrate Z-GGL-AMC; and direct visualization of proteasome activity in living cells that stably express the short-lived proteasome activity sensor protein Ub^{G76V}–GFP (Dantuma et al., 2000).

N_2a-M cells were incubated for 16 hours with 30 μg/ml CsA, 75 μM ALLN or left untreated. The cells were lysed, cleared by centrifugation and subjected to an in vitro proteasome activity assay. Fluorescence emission of the released AMC was measured in 3-minute intervals for 1 hour. Similar fluorescence increase rates, reflecting indistinguishable proteasome activity levels, were observed in untreated (Fig. 2A, diamonds) and in CsA-treated (Fig. 2A, triangles) cells. By contrast, nearly no fluorescence was detected in the ALLN-treated cell homogenates (Fig. 2A, squares). These observations indicate that CsA does not impair proteasome activity of the cell population.

Next, we measured proteasome activity in live CHO cells stably expressing the proteasome activity sensor Ub^{G76V}–GFP. Fluorescence levels were visualized in cells that were treated for 24 hours with either 30 μg/ml CsA, 30 μM ALLN or left untreated. In both untreated and CsA-treated cells, no GFP signal could be detected (Fig. 2B, panels IV and VI, respectively), whereas a bright GFP signal was seen in the ALLN-treated cells (Fig. 2B, panel V).

To assess the possibility that CsA treatment does inhibit the proteasome and also prevents Ub^{G76V}–GFP from reaching its fluorescence-emitting conformation, we measured the amount of Ub^{G76V}–GFP within the cells by western blot with a GFP antibody. CHO-Ub^{G76V}–GFP cells were left untreated or incubated for 24 hours with either 30 μM or 60 μM ALLN, or 15 μg/ml or 30 μg/ml CsA. Our results clearly indicated that Ub^{G76V}–GFP accumulated as a result of ALLN in a dose-dependent manner (Fig. 2C, lanes 2 and 3), but not in response to CsA treatment (Fig. 2C. lanes 4 and 5). These observations confirmed that the CsA treatments used in our experiments have no effect on proteasome activity in the cell population.

Because only a fraction of the cells in CsA-treated culture contain PrP aggresomes (Cohen and Taraboulos, 2003), it is possible that these deposition sites are formed solely in cells that exhibit reduced proteasome activity or in cells that massively overexpress PrP. In this scenario, the formation of the PrP aggresomes is a consequence of proteasome overload in specific cells and is thus undetectable at the population level. We tested this possibility by transiently transfecting CHO-Ub^{G76V}–GFP cells with the MHM_2 PrP chimera. Twenty-four hours after transfection, the cells were incubated with either 30 μg/ml CsA or 60 μM ALLN for an additional 24 hours and subjected to immunofluorescence using a PrP antibody (Fig. 2D, red channel). Whereas GFP fluorescence was seen in ALLN-treated cells (Fig. 2D, panel III), no GFP signal could be detected in CsA-treated PrP-aggresome-containing cells (Fig. 2D, panel IV). These results show that proteasome activity is intact in cells containing CsA–PrP aggresomes.

PrP molecules within the aggresomes are mobile

Chaperone and proteasome recruitment to the CsA–PrP aggresomes suggests that these structures serve as dynamic quality-control compartments in which a continuous process of disaggregation and PrP clearance can occur. This would require molecular mobility within the aggresome, and a constant exchange of PrP molecules between the aggresome and the cytosol.

In order to investigate the dynamics and localization of the aggresome-resident PrP molecules, we expressed YFP–PrP in live cells (supplementary material Fig. S4A). First, we tested whether the YFP–PrP protein accumulates in aggresomes following CsA treatment. Cells stably expressing the YFP–PrP chimera (CHO-YFP–PrP cells) were treated with 60 μg/ml CsA for 16 hours. Immunofluorescent microscopy indicated that the YFP–PrP

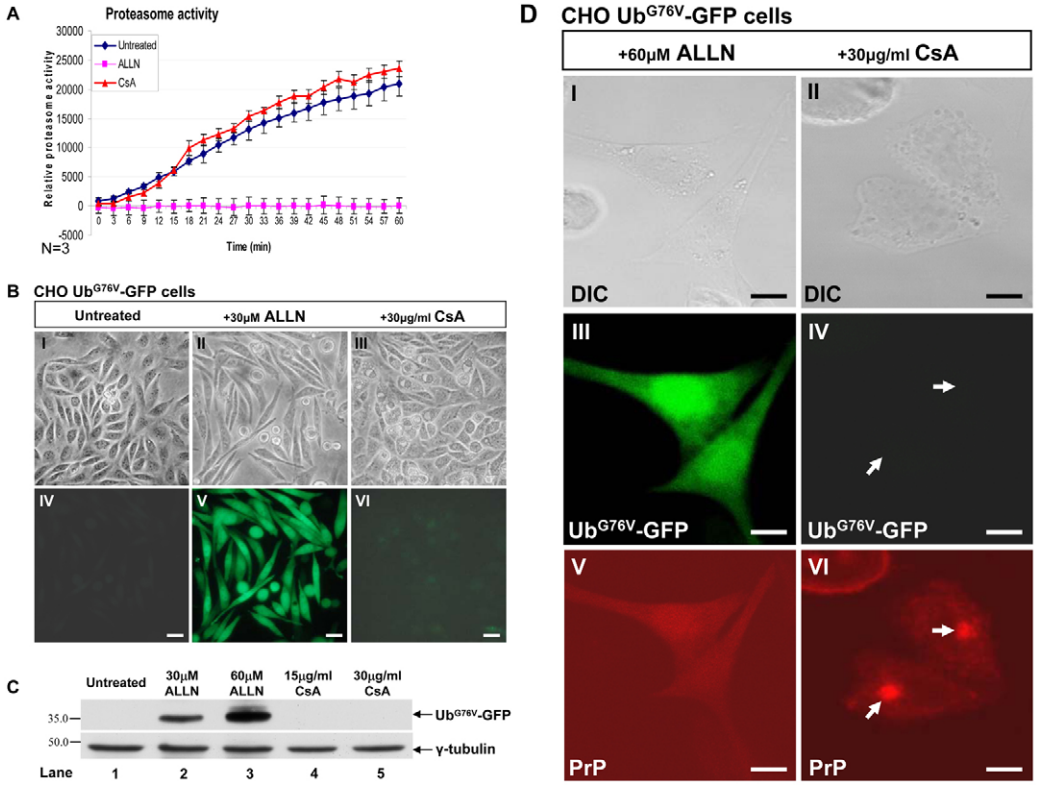

Fig. 2. Intact proteasome activity in CsA-treated cells. (**A**) N_2a-M cells were treated with either 30 μg/ml CsA or 75 μM ALLN, or left untreated. The cells were lysed and the same concentrations of the drugs were added to the PNS with the fluorogenic chemotrypsin-like proteasome activity sensor Z-GGL-AMC. Similar fluorescence emission (435 nm) increase rates were measured in untreated (diamonds) and CsA-treated (triangles) cell lysates, indicating similar rates of proteasome activity. No fluorescence was detected in lysates of cells treated with ALLN (squares). (**B**) No GFP signal was detected in living CHO cells stably expressing Ub^{G76V} –GFP that were left untreated or treated with 30 μg/ml CsA (panels IV and VI, respectively), indicating intact proteasome activity. By contrast, bright GFP signal was detected in cells treated with 30 μM ALLN (panel V). Scale bars: 5 μm. (**C**) CHO-Ub^{G76V}–GFP cells were either left untreated or treated for 24 hours with either 30 μM or 60 μM ALLN, or with 15 μg/ml or 30 μg/ml CsA (lanes 1–5, as indicated). Western blot analysis revealed Ub^{G76V}–GFP bands in the ALLN-treated cells (lanes 2 and 3), but not in untreated (lane 1) or CsA-treated cells (lanes 4 and 5). (**D**) Plasmid carrying the PrP-MHM_2 gene was transiently transfected into CHO cells that stably express Ub^{G76V}–GFP. The cells were treated with either 30 μg/ml CsA or 60 μM ALLN for 24 hours and then subjected to immunofluorescence using PrP antibody (panels V and VI). Unlike in ALLN-treated cells (panel III), no GFP signal could be detected in over 50 aggresome-containing cells (panel IV). Arrows point at CsA–PrP aggresomes. Scale bars: 3 μm.

molecules accumulated in juxta-nuclear deposits (supplementary material Fig. S4B, panel I) and colocalized with PrP antibody staining (supplementary material Fig. S4B, panels II and III). These YFP–PrP deposits also colocalized with the MTOC (supplementary material Fig. S4C, arrows), a hallmark feature of aggresomes (Johnston et al., 1998), confirming that, similar to wild-type PrP, the fluorescent YFP–PrP molecules accumulate in aggresomes upon CsA treatment. Western blot analysis using a PrP antibody indicated that, similar to the amounts of PrP-MHM_2 expressed in CHO-M cells, the expression level of YFP–PrP in CHO-YFP–PrP cells is moderate (supplementary material Fig. S4D).

The rate of molecular mobility within the JUNQ and IPOD deposits is a key difference between these aggregate deposition sites. Whereas molecules residing within the JUNQ compartment are mobile, IPOD-resident molecules are not (Kaganovich et al., 2008). In order to better define the PrP aggresome, we sought to characterize the mobility of molecules residing within these structures by using the fluorescence recovery after photobleaching (FRAP) assay. This technique is based on a high-power laser pulse, which bleaches the fluorescent signal of affected molecules in a limited area within the examined compartment, followed by a kinetic analysis of the signal recovery (Lippincott-Schwartz et al., 2003). We subjected CsA-treated CHO-YFP–PrP cells to FRAP, bleaching a small aggresomal area, and observed rapid recovery of the bleached area (Fig. 3A, insets). Quantification of the fluorescence intensity within the bleached area revealed that it recovered from 45% to approximately 80% of its original signal within 110 seconds (Fig. 3B, data were normalized to the intensity loss of unbleached neighboring aggresomes). This set of experiments indicated that, like JUNQ-resident molecules, YFP–PrP molecules in the aggresomes are highly mobile.

Proteasomes mediate the clearance of aggresome-resident PrP molecules

If the UPS mediates the turnover of aggresome-resident PrP molecules, fast molecular exchange between the aggresome and the cytosol is expected. Such rapid exchange is a feature of dynamic quality-control compartments such as the JUNQ but not of the IPOD (Kaganovich et al., 2008). Thus, we sought to test whether the PrP aggresomes exchange molecules with the cytosol by employing the fluorescence loss in photobleaching (FLIP) technique (Lippincott-Schwartz et al., 2003). Briefly, this method is based on continuous bleaching of a small cytosolic area outside of the aggresome by a laser beam. This leads to the bleaching of cytosolic

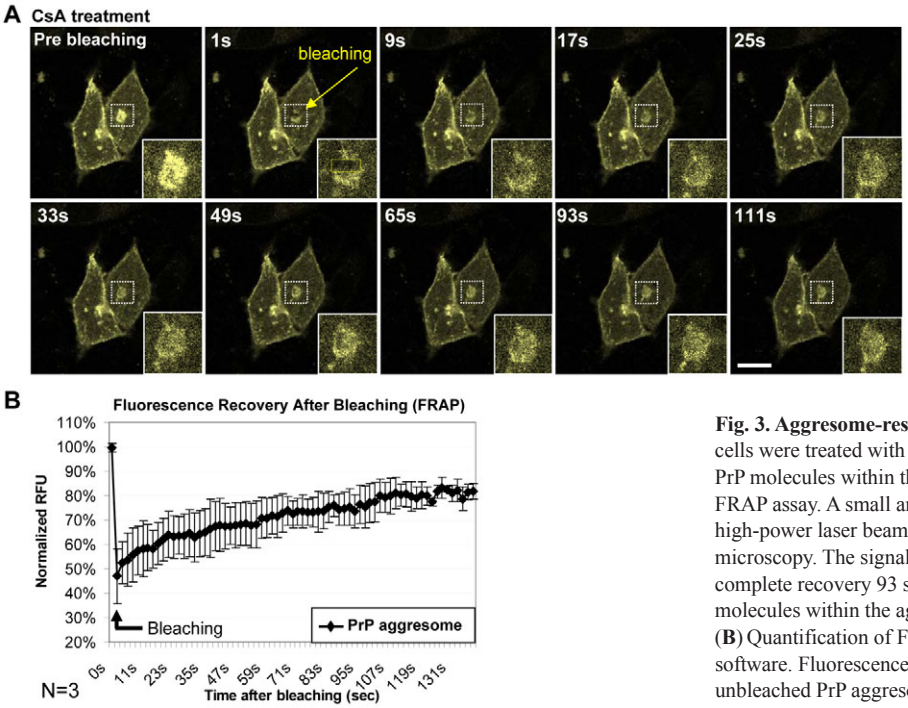

Fig. 3. Aggresome-resident PrP molecules are mobile. (**A**) CHO-YFP–PrP cells were treated with 60 μg/ml CsA for 16 hours and the mobility of YFP–PrP molecules within the YFP–PrP aggresome was tested in living cells using FRAP assay. A small area within a YFP–PrP aggresome was bleached by a high-power laser beam and the fluorescent recovery was followed by confocal microscopy. The signal within the bleached area (insets) exhibited nearly complete recovery 93 seconds after bleaching, indicating that YFP–PrP molecules within the aggresomes are highly mobile. Scale bar: 3 μm. (**B**) Quantification of FRAP dynamics using ImageJ image processing software. Fluorescence levels were normalized to those of neighboring unbleached PrP aggresomes (*n*=3).

YFP–PrP molecules prior to their transport into the aggresome, thus depleting the aggresome of fresh fluorescent PrP molecules. Molecules that move from the aggresomes to the cytosol lose their fluorescence as well. The rate of fluorescence loss as a function of time correlates with the rate of molecule exchange between the compartment of interest and the cytosol. We subjected CsA-treated CHO-YFP–PrP cells to FLIP and found that constant cytosolic bleaching resulted in a rapid decline of the aggresome fluorescent intensity (Fig. 4A). Comparative quantification of the signal within the aggresome and of unbleached cytosolic area revealed that the normalized rates of fluorescence decline in the aggresome and the cytosol were indistinguishable (Fig. 4C). The rate of fluorescence decline was much faster in PrP-containing vesicles that appear following treatment with the proteasome inhibitor MG132 (supplementary material Fig. S5), confirming that proteasome inhibition and CsA treatment lead to the accumulation of misfolded PrP molecules in distinct types of inclusions. Together, these results indicate that the CsA–PrP aggresome is a dynamic structure that rapidly exchanges molecules with the cytosol.

The accumulation of proteasomes in close proximity to PrP aggresomes (Cohen and Taraboulos, 2003) and the activity of intact proteasomes in cells containing CsA–PrP aggresomes (Fig. 2D) further suggest that proteasomes might play an active role in degrading aggresome-resident misfolded PrP molecules. To examine this possibility, we treated CHO-YFP–PrP cells with 60 μg/ml CsA for 18 hours and supplemented the cell media with 10 μM MG132 (altogether the cells were exposed to CsA for 24 hours and to MG132 for the last 6 hours). Aggresome-containing cells were subjected to the FLIP assay as described above. If proteasomes facilitate the degradation of aggresome-resident YFP–PrP, it is expected that proteasome inhibition will slow the degradation rate of these molecules and, in turn, stabilize the fluorescent signal of the aggresomes. If proteasomes play no role in clearing the aggresome-resident YFP–PrP molecules, proteasome inhibition will have no effect on the intensity of the fluorescent signal detected in aggresomes. Our results (Fig. 4B) clearly demonstrate that proteasome inhibition slowed the rate of decline of the aggresome-specific fluorescent signal (compare Fig. 4A and 4B). Signal quantification indicated that, when proteasomes were fully active, the normalized fluorescent signal detected in the FLIP experiment reached about 21% of its original level after one minute (Fig. 4C, black line). By contrast, when proteasomes were inhibited, the signal intensity was approximately 55% of the original level at the same time point (Fig. 4D, black line). The cytosolic fluorescent signal was bleached at similar rates in the absence and presence of MG132 (compare Fig. 4C and 4D, red lines). Similar results were obtained when ALLN was used to inhibit proteasomes (supplementary material Fig. S6).

Maintaining the stability of the aggresome while rapidly exchanging molecules with the cytosol requires a constant YFP–PrP influx into this structure. Thus, we predicted that preventing the supply of new misfolded YFP–PrP molecules into the aggresome will lead to its disintegration and disappearance, whereas proteasome inhibition will cause stabilization by the accumulation of YFP–PrP molecules in the aggresome. To test this, we treated CHO-YFP–PrP cells with CsA for 16 hours, supplemented the cell media with either 20 μg/ml cycloheximide (CHX) (an inhibitor of protein translation) or 20 μM MG132, and followed YFP–PrP aggresomes for 9 hours using live confocal imaging. Whereas CsA–PrP aggresomes of cells treated solely with CsA were stable for the entire course of the experiment (Fig. 4E, CsA), blocking translation resulted in disintegration of the aggresomes (Fig. 4E, CsA+CHX). By contrast, CsA–PrP aggresomes of cells treated with MG132 exhibited constant enlargement and a more intense signal, indicating accumulation of YFP–PrP molecules within the aggresome (Fig. 4E, CsA+MG132). Quantification of three aggresomes per treatment confirmed our observations (Fig. 4F).

Together these observations indicate that CsA–PrP aggresomes are dynamic structures in which aggregated misfolded YFP–PrP

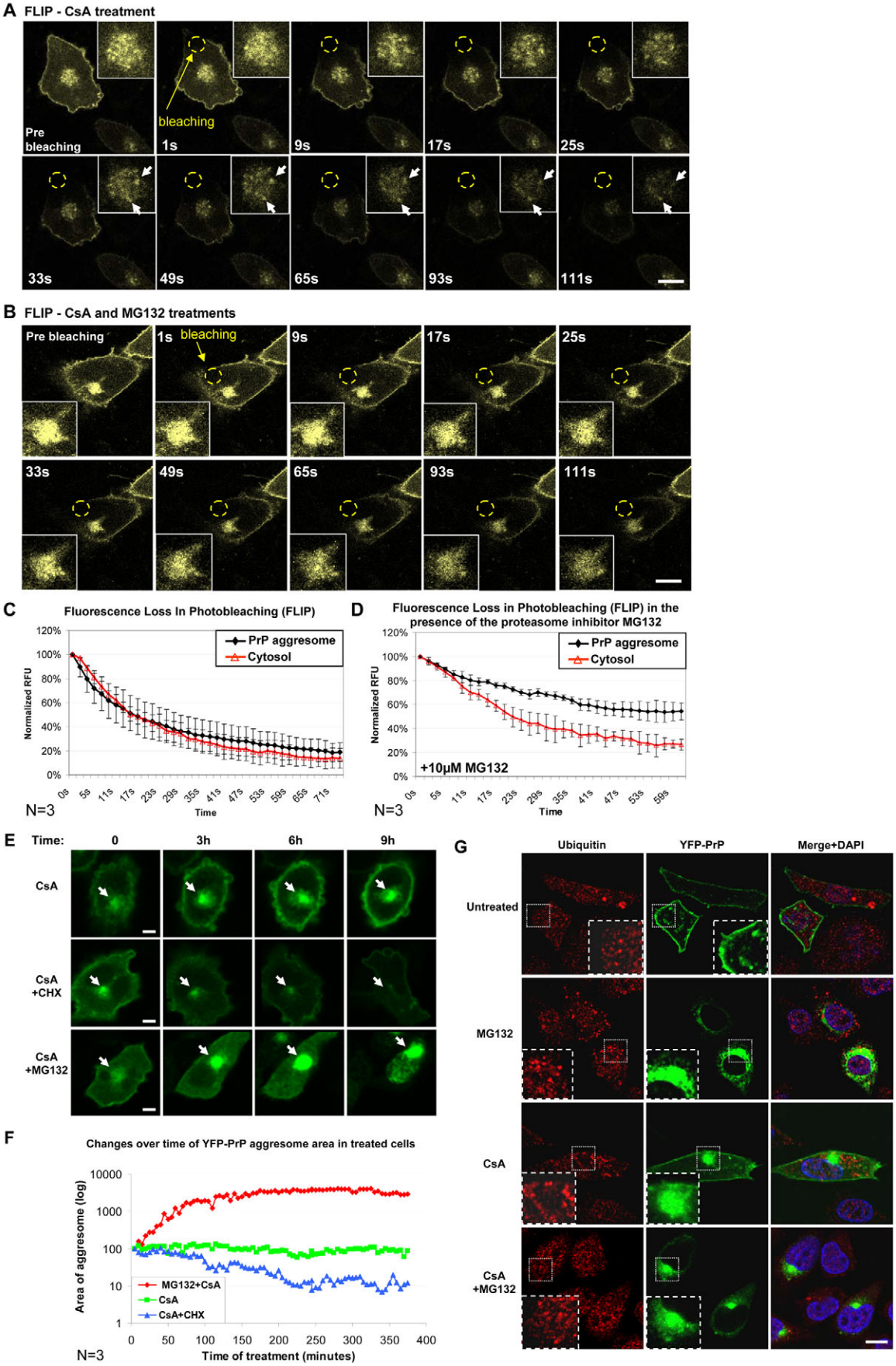

Fig. 4. See next page for legend.

molecules constantly accumulate and undergo degradation by proteasomes.

The degradation of aggresome-resident PrP molecules by the UPS suggests that proteasome inhibition will result in the accumulation of ubiquitylated PrP molecules in the aggresome. To test this hypothesis, we treated CHO-YFP–PrP cells with either CsA (for 18 hours) or MG132 (for 5 hours), or with both CsA (for 18 hours) and MG132 (added during the last 5 hours of CsA treatment), as described above. The cells were subjected to immunofluorescence assay using two different ubiquitin antibodies. No ubiquitin signal could be detected in CsA–PrP aggresomes of cells treated with either CsA alone (Fig. 4G, CsA) or with CsA and MG132 (Fig. 4G, CsA+MG132). The lack of ubiquitin signal in YFP–PrP aggresomes was corroborated by colocalization analysis of the images (supplementary material Fig. S7). Similar results were obtained when a different ubiquitin antibody was used (supplementary material Fig. S8). Even though the absence of ubiquitin signal in CsA–PrP aggresomes is consistent with our previous observation (Cohen and Taraboulos, 2003), a similar experimental approach revealed that PrP^{Sc} aggresomes contain ubiquitylated proteins (Kristiansen et al., 2005). Although our observations suggest that aggresome-resident CsA–PrP molecules are degraded by proteasomes in a ubiquitin-independent pathway, further research is needed to characterize this mechanism.

CsA–PrP aggresomes and IPODs exhibit different properties

The attraction of molecular chaperones, high internal molecular mobility and rapid exchange rate with the cytosol are all characteristics that define the CsA–PrP aggresome as a JUNQ-like deposition site. To further establish the definition of PrP aggresomes as dynamic quality-control compartments, we sought to directly test whether they are distinct from the IPOD. For this purpose, we employed a modified fluorescence protease protection (FPP) assay (Lorenz et al., 2006). The IPOD-resident fluorescently tagged protein HttQ97–RFP (Kaganovich et al., 2008) exhibits elevated resistance to solubilization and proteolysis compared with the JUNQ-resident protein ChFP–VHL (S. J. Weisberg et al., unpublished). CHO cells harboring IPOD containing HttQ97–RFP, JUNQ containing ChFP–VHL or YFP–PrP aggresomes were incubated for 140 seconds with 120 μM digitonin and the integrities of the fluorescent deposition sites were tracked over time. Next, 500 μM trypsin was added and the integrities of the fluorescent cellular deposition sites were recorded. Our results (Fig. 5) indicate that, whereas the HttQ97–RFP IPODs exhibited resistance to the digitonin and trypsin treatment, the YFP–PrP within aggresomes was digested in a similar manner to JUNQ-resident ChFP–VHL [the digestion of IPOD-resident HttQ97–RFP molecules was achieved only by the addition of proteinase K (PK)] (Fig. 5). These observations indicate that CsA–PrP aggresomes are distinct from the IPOD structure, and share their detergent and proteolysis sensitivity with the JUNQ compartment.

More than one misfolded PrP population is present within aggresomes

Detailed examination of the aggresomes of cells subjected to FLIP analysis revealed that some areas within the aggresomes exhibited relative resistance to the bleaching process (Fig. 4A, bottom panels, insets, arrows). This observation suggests that more than one YFP–PrP subpopulation exists in the aggresome – one that is rapidly degraded by proteasomes and one that exhibits relative stability. To further test this possibility, we treated six plates of N2a-M cells with 60 μM ALLN and six other plates with 25 μg/ml CsA for 16 hours and then replaced the cell media with fresh media. Right after the removal of the drugs (day 0) and every 24 hours thereafter, cells from one plate of each treatment were collected, lyzed and cleared by low-speed centrifugation. We tested the relative stability of PrP in the CsA- and ALLN-treated cells by treating the cleared lysates for 20 minutes with 20 μg/ml PK. The presence of aggregated, PK-resistant PrP species is correlated with toxicity and prion disorders (Peretz et al., 2002). PK-resistant PrP molecules have been also shown to accumulate in cells following proteasome inhibition (Ma and Lindquist, 2001; Yedidia et al., 2001) and CsA treatment (Cohen and Taraboulos, 2003). The amounts of PK-resistant PrP molecules were analyzed using western blotting against PrP. As expected, PK-resistant PrP molecules accumulated in cells exposed to both treatments (Fig. 6A); however, whereas three days after the removal of ALLN, no PK-resistant PrP could be observed, PK-resistant PrP bands were detected in the CsA-treated cells as many as five days after the removal of the drug (Fig. 6A, bottom panel). High-pressure liquid chromatography (HPLC) analysis confirmed that CsA was removed from the cells by rinses and media replacement (supplementary material Fig. S9). Importantly, comparing the PK-resistant PrP content immediately after CsA removal (Fig. 6A, bottom panel, lane 1) and 24 hours later (Fig. 6A, bottom panel, lane 2) revealed that the majority of PK-resistant PrP molecules were cleared within the first day after CsA removal. This observation supports the hypothesis that more than one misfolded PrP subpopulation is present within CsA-treated cells and suggests that at least a fraction of the CsA-aggresome-resident PrP molecules exhibit a remarkable resistance to proteolysis. These results raise the prospect that CsA–PrP aggresomes are needed after the removal of

Fig. 4. YFP–PrP aggresomes rapidly exchange molecules with the cytosol. Proteasomes mediate the degradation of aggresome-resident YFP–PrP molecules. (**A**) FLIP assay indicated that YFP–PrP aggresomes rapidly exchange molecules with the cytosolic pool, as reflected by massive fluorescence loss within 93 seconds (insets). The signal of specific areas within the aggresome exhibited relative resistance (lower panels, insets, arrows). (**B**) To evaluate whether proteasomal degradation underlies the rapid decline in the intensity of fluorescent signal within YFP–PrP aggresomes, CHO-YFP–PrP cells were treated for 18 hours with 60 μg/ml CsA, supplemented with 10 μM MG132 and incubated with both drugs for an additional 5 hours. FLIP assay indicated that proteasome inhibition results in a slower decline of the fluorescent signal within aggresomes compared with the cytosolic signal (insets). (**C**) Quantitative analysis of three FLIP experiments revealed that the rates of loss of aggresomal and cytosolic fluorescent signals were nearly identical. (**D**) Quantification of the fluorescent signals in YFP–PrP aggresomes and in the cytosol of cells treated with CsA and MG132, as indicated in B. Aggresome signal intensity declined to approximately 55% of its original level within one minute, while at the same time point the cytosolic signal declined to about 25% of its level at the beginning of the experiment. (**E**) Although the size of aggresomes in CsA-treated cells was stable over time (CsA), the inhibition of translation by the addition of 10 μg/ml CHX to the media of CsA-treated cells (CsA+CHX) leads to disintegration of YFP–PrP aggresomes. By contrast, proteasome inhibition using MG132 (CsA+MG132) resulted in constant enlargement of the YFP–PrP aggresome. (**F**) Quantification of aggresomes (pixel area above threshold) treated as in E. (**G**) No ubiquitin staining (red channel, DAKO antibody) could be detected colocalizing with YFP–PrP aggresomes (green channel) of CHO-YFP–PrP cells treated with CsA. Partial colocalization was seen in cells treated with both CsA and MG132 [nuclei were labeled with DAPI (blue)]. Scale bars: 3 μm.

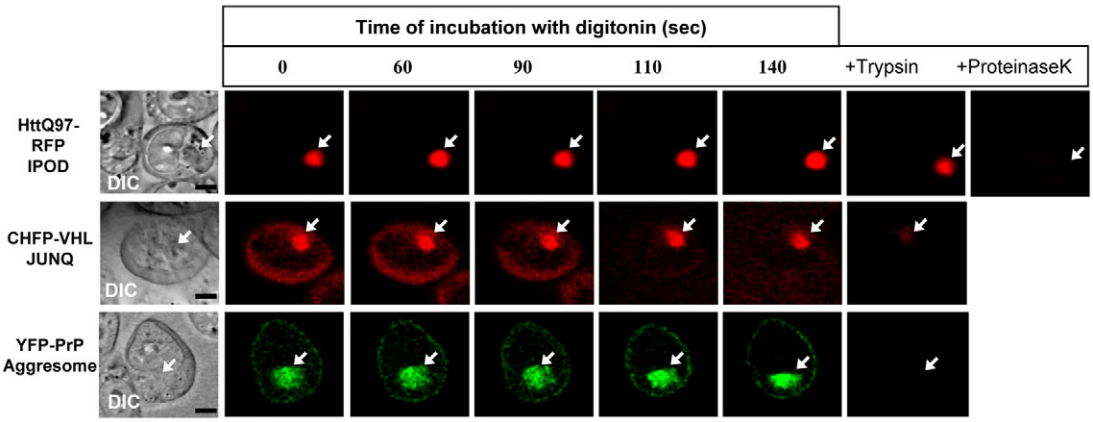

Fig. 5. CsA–PrP aggresomes are distinct from IPOD. A modified FPP assay indicated that, similarly to JUNQ-resident ChFP–VHL molecules, aggresome-resident YFP–PrP molecules exhibit increased sensitivity to proteolysis compared with IPOD-resident HttQ97–RFP. Digestion of the IPOD-resident HttQ97–RFP molecules could be achieved by PK. Arrows point at aggregate deposition sites (IPOD, JUNQ or YFP–PrP aggresome).

CsA in order to confine the stable CsA–PrP species, which might have more considerable hazardous potential. To assess this hypothesis and track the stability of PrP aggresomes in the absence of CsA, we employed time-lapse confocal microscopy on live CHO-YFP–PrP cells that were rinsed and supplied with fresh media following incubation with 60 μg/ml CsA for 16 hours. Aggresome-containing cells were tracked for an additional 16 hours subsequent to media replacement. Aggresomes from multiple cells exhibited stability; they were detectable through the entire course of the experiment despite the removal of CsA (Fig. 6B, arrows).

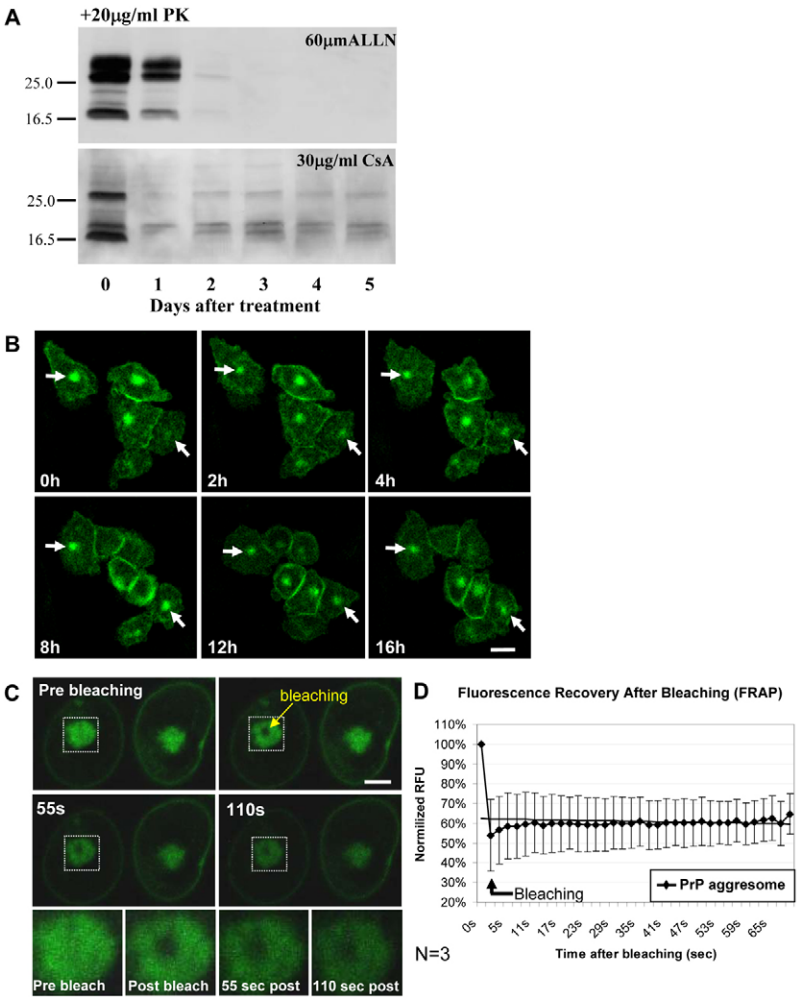

Fig. 6. YFP–PrP aggresomes are stable structures that contain more than one PrP subpopulation. (**A**) N2a-M cells were treated for 16 hours with either 60 μM ALLN or 30 μg/ml CsA. The drugs were removed by replacing the media and one plate of cells per treatment was collected and lysed in 24 hour intervals for five consecutive days after removal of the drugs. Lysates were cleared by centrifugation and the PNS was treated for 20 minutes with 20 μg/ml PK and analyzed by western blot. PK-resistant PrP molecules could be seen in CsA-treated cells through the course of the experiment, but were not detectable in ALLN-treated cells three days after the removal of the drug. (**B**) CHO-YFP–PrP cells were treated for 16 hours with 60 μg/ml CsA, the cell medium was replaced and aggresome-containing cells were visualized and photographed for an additional 16 hours in 30 minute intervals. CsA–PrP aggresomes were found to be stable during the entire course of the experiment (arrows). Scale bar: 5 μm. (**C**) CHO-YFP–PrP cells were treated with 60 μg/ml CsA for 24 hours, the cell medium was replaced and the cells were incubated with fresh media for an additional 32 hours. The mobility of YFP–PrP molecules within PrP aggresomes was tested in living cells using FRAP assay. A small area within an YFP–PrP aggresome was bleached by a high-power laser beam and the fluorescent recovery was followed by confocal microscopy. The signal within the bleached area (insets) did not recover 110 seconds after bleaching, indicating that YFP–PrP molecules within the aggresomes are less mobile than those within aggresomes in constantly treated cells. Scale bar: 3 μm. (**D**) Quantification of FRAP dynamics using ImageJ image processing software. Fluorescence levels were normalized to those of neighboring unbleached PrP aggresomes (n=3).

The finding that CsA–PrP aggresomes are relatively stable after the removal of CsA raised the question of whether the properties of the molecular content of the aggresomes change over time. In the IPOD, molecular stability is correlated with low mobility (Kaganovich et al., 2008). Thus, we employed the FRAP assay and examined whether molecular mobility within aggresomes that remain after the removal of CsA ('lasting aggresomes') changed over time. CHO-YFP–PrP cells were treated for 24 hours with CsA to induce the formation of PrP aggresomes, the cell medium was replaced with fresh medium and the cells were incubated for additional 32 hours prior to FRAP assay. Our results (Fig. 6C) indicated that the YFP–PrP molecules within the lasting aggresomes were less mobile than those within aggresomes that were present in cells that were constantly exposed to CsA (compare Fig. 3A and Fig. 6C). Signal quantification indicated that, 69 seconds after bleaching, the signal recovery rate within constantly treated aggresomes was approximately 30% (Fig. 3B), whereas less than 10% recovery was measured in lasting aggresomes within the same period of time. This observation corroborates the notion that aggresomes contain more than one PrP subpopulation.

Discussion

The results presented in this study show that CsA-induced PrP aggresomes are dynamic structures that attract chaperones, rapidly exchange PrP molecules with the cytosol and have no detectable effect on proteasome activity. Similarly to JUNQ, but unlike the IPOD, PrP aggresomes attract proteasomes and exhibit sensitivity to trypsin digestion. Together, our observations demonstrate that CsA–PrP aggresomes are functionally homologous to the recently described JUNQ compartment and serve as dynamic quality-control centers where misfolded, aggregated PrP molecules accumulate and are prepared for degradation. Interestingly, whereas a recent report shows that a yeast prion-like protein accumulates in the IPOD (Tyedmers et al., 2010), our discoveries suggest that dynamic quality-control compartments can contain disease-linked misfolded protein aggregates, implying a protective role for the JUNQ-like CsA aggresome. Thus, it is probable that protein aggregates are sorted to the appropriate compartment according to their aggregation state and the cellular ability to degrade them.

Cellular pathways of PrP processing

In intact cells, the folding of newly synthesized PrP molecules is assisted by chaperones, including members of the cyclophilin family (Fig. 7, step 1). The molecules then undergo modifications (Fig. 7, step 2) and are transported to the plasma membrane (Fig. 7, step 3). Despite the activity of chaperones, a fraction of these molecules fail to fold properly (Fig. 7, step 4), undergo ubiquitylation and are directed to proteasomal degradation (Fig. 7, step 5). When CsA is added to the cells (Fig. 7, step 6), at least two unfolded PrP subpopulations are formed and accumulate in the aggresome (Fig. 7, step 7). One subpopulation is relatively sensitive and thus is quickly prepared by chaperones and digested by the proteasomes (Fig. 7, step 8). However, the other type of aggresome-resident PrP molecule exhibits relative proteasome resistance and stability. If this subpopulation is in fact degraded by proteasomes, it is by a slower process (Fig. 7, step 9).

How do CsA-induced misfolded PrP molecules escape degradation?

It has been previously shown that the treatment of PrP-expressing cells with proteasome inhibitors, such as ALLN, MG132 or lactacystin, induces the accumulation of ubiquitylated, insoluble PrP species (Ma and Lindquist, 2001; Yedidia et al., 2001). However, when the UPS is fully active, these PrP molecules undergo constant degradation by proteasomes. Interestingly, proteasome inhibition results in PrP aggresome formation exclusively in cells overexpressing disease-linked, mutated PrP molecules, but not in cells overexpressing wild-type PrP (Cohen and Taraboulos, 2003; Mishra et al., 2003). These findings suggest that UPS impairment induces the formation of aggresomes only on a background of highly aggregated misfolded PrP molecules, which might correlate with their toxic potential. Thus, it was expected that CsA treatment would result in a dual effect: the induction of PrP misfolding, creating aggregation-prone conformers, and proteasome impairment, enabling the accumulation of these PrP species in aggresomes. The observation that aggresomes containing PrP^{Sc} impair proteasome activity (Kristiansen et al., 2007) further predicts that CsA–PrP aggresomes inhibit the UPS. Surprisingly, we discovered that CsA treatment induces the accumulation of

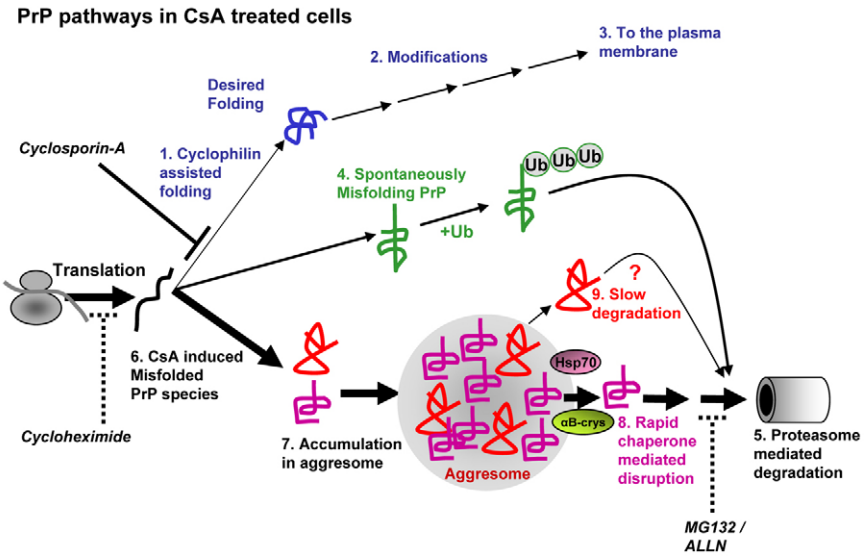

Fig. 7. Cellular PrP processing pathways – a model. Cyclophilin-assisted PrP folding (step 1) ensures correct structure and proper maturation (steps 2 and 3) in intact cells. However, a fraction of the newly synthesized PrP molecules fail to fold properly (step 4), undergo ubiquitylation and are directed to proteasomal degradation (step 5). In the presence of CsA, at least two unfolded PrP subpopulations are formed (step 6) and accumulate in the aggresome (step 7) – a sensitive subpopulation that is digested by the proteasomes (step 8) and a proteasome-resistant PrP subpopulation that is slowly degraded by proteasomes, if at all (step 9).

misfolded wild-type PrP in aggresomes despite intact proteasome activity, raising the question of how CsA–PrP molecules escape, or at least are delayed from, UPS-mediated degradation. One possibility is that CsA treatment leads to the formation of PrP conformers that form highly stable structures that are inaccessible to the UPS. This hypothesis suggests that, like the mutated PrP P102L and PrP P105L, CsA–PrP forms a highly stable prion seed that leads to GSS development (Cohen and Taraboulos, 2003). An alternative explanation is that the degradation rate of the CsA–PrP species is slower than their formation rate, enabling accumulation, aggregation and the formation of CsA–PrP aggresomes. It is plausible that the confinement of these potentially toxic PrP species in aggresomes sequesters them from the cytosolic environment, prevents cellular damage and facilitates their slow degradation by the UPS.

The observation that, similarly to other types of aggresomes (Garcia-Mata et al., 1999), PrP aggresomes attract proteasomes but exhibit no detectable ubiquitin staining (Cohen and Taraboulos, 2003) points to the possibility that ubiquitylation is the rate-limiting step in the UPS-mediated degradation of CsA–PrP molecules. However, the intact ubiquitylation in CsA-treated cells (Cohen and Taraboulos, 2003) and the absence of colocalized detectable ubiquitin signal with the CsA–PrP aggresomes of cells treated with both CsA and proteasome inhibitor (Fig. 4G; supplementary material Fig. S8) might imply a ubiquitin-independent degradation mechanism. Ubiquitin-independent proteasome-mediated protein degradation of aggresome-resident (Garcia-Mata et al., 1999) and non-aggresome-resident proteins was reported previously (Bercovich et al., 1989; Rosenberg-Hasson et al., 1989; Stewart et al., 2010). Moreover, proteasomes digest the PD-linked aggregative protein α-synuclein in a ubiquitin-independent manner (Tofaris et al., 2001). Perhaps the unique structure of CsA–PrP molecules leads to their degradation in an unconventional pathway that exhibits a slower activity rate, enabling the accumulation and aggregation of the CsA–PrP molecules without affecting the clearance rates of other PrP species and of other UPS substrates. A third possibility suggests that disaggregation might be the rate-limiting activity that slows the degradation of CsA–PrP. We recently reported that disaggregation, which is essential to enable the degradation of aggregated Alzheimer's associated peptide Aβ, is carried out by specialized machinery that exhibits no detectable proteolytic activity (Bieschke et al., 2009). Although it is unknown what cellular components mediate CsA–PrP disaggregation, it is possible that specialized cellular chaperones execute this activity (Behrends et al., 2006; Shorter and Lindquist, 2004). We found that aggregate-disrupting small heat shock proteins (reviewed by Hartl and Hayer-Hartl, 2002) and Hsp70 colocalized with CsA–PrP aggresomes. These chaperones were also found to be recruited to aggresomes containing other types of misfolded proteins (Garcia-Mata et al., 1999). These findings suggest that the universal chaperone machinery disrupts toxic aggregates of different proteins and prepares them for degradation.

Possible links between PrP aggresomes, aging and prion disorders

We previously reported that, like other disease-linked PrP mutants (Mishra et al., 2003), the proline-substituted PrP molecules accumulate in aggresomes exclusively when proteasomes are inhibited (Cohen and Taraboulos, 2003). The apparent similarity between GSS-associated mutated PrP overexpression and CsA treatment raises the following question: why is overexpression of disease-linked PrP mutants not sufficient for aggresome formation (even in cells with a fully active UPS)? One possible explanation is that CsA has a broader deleterious effect on the cellular counter-aggregation mechanism, in addition to the inhibition of proper PrP folding. Such additional effects might result from the inhibition of cyclophilins, chaperones that play roles in the maturation of disaggregation- or degradation-mediating proteins. In this view, the aggregate clearance capabilities of untreated cells are more similar to those exhibited by cells of young organisms in which disaggregation and degradation efficiently clear aggregated proteins, whereas CsA-treated cells mimic the capabilities of old organisms in which such protective activities are compromised (Balch et al., 2008). We reported previously that reduced disaggregation activity is associated with aging in nematodes (Cohen et al., 2006). The finding that the manipulation of aging through the insulin-like growth factor 1 (IGF1) signaling pathway delays the onset of AD-like disease in aged mice (Cohen et al., 2009; Freude et al., 2009) supports this theory. It is tempting to speculate that aggresome formation is a secondary defense mechanism, initiated in old cells that suffer from reduced aggregate clearance capabilities. An organismal aging model will be required to test this hypothesis.

Our study provides new insights into the protective roles of aggresomes as a component of the cellular counter-aggregation mechanism. It suggests that aggresomes help cells sequester small toxic PrP species that cause infectious prion disorders (Silveira et al., 2005) and mediate their degradation. Better understanding of aggresome formation and its relation to the aging process will be beneficial towards the development of novel neurodegeneration therapies.

Materials and Methods

Materials

Cell culture reagents were purchased from Biological Industries (Beit Haemek, Israel). G-418 and Z-GGL-AMC (539144) were purchased from Calbiochem (San Diego, CA). Protein concentration was determined using BCA kit (Pierce 23223). CsA (C1832), CHX (C7698), MG132 (C2211) and ALLN (A6185) and all other reagents were from Sigma.

Cell cultures and transfections

N_2a-M and CHO-M cells stably express moderate levels of the MHM_2-PrP chimeric protein (Scott et al., 1992). CHO-YFP–PrP cells stably express the YFP–PrP chimera. Cells were grown at 37°C in DMEM supplemented with 10% fetal calf serum. For the PK resistance experiment, low-glucose DMEM16 medium was used. Stable transfections were achieved with the reagent FuGENE 6 (Roche, #1-814-443) according to the manufacturer's instructions. Selections were performed using G-418 (1 mg/ml for N_2a and 0.75 mg/ml for CHO cells).

Plasmids

The PrP-MHM_2 plasmid is described elsewhere (Scott et al., 1992). The Ub^{G76V}–GFP plasmid was a generous gift of Dr Nico Dantuma (Department of Cell and Molecular Biology, Karolinska Institute, Stockholm, Sweden). YFP–PrP chimera was based on the pSPOX plasmid. YFP was inserted into the sequence of the PrP-MHM_2 chimera (Scott et al., 1992) between residues 28 and 29. pcDNA3.1-mCherry-VHL and pcDNA3.1-HttQ97-mRFP3.1 plasmids are described in Kaganovich et al. (Kaganovich et al., 2008).

Antibodies

MHM_2-PrP was detected using either the rabbit antiserum R073 (Serban et al., 1990) or the mouse monoclonal antibody 3F4 (SIG-39600), which was purchased from Covance (Princeton, NJ). Mouse monoclonal anti-ubiquitin antibody (MMS-258R) was from Babco (Richmond, CA) and rabbit polyclonal anti-ubiquitin antibody (Z0458) from Dako cytomation. Rabbit PrP antiserum (RO73) was used for western blot (1:5000) or for immunofluorescence (1:1200). γ-Tubulin monoclonal antibody was from Sigma (T6557); Hsp40 antiserum (SPA-400), Hsp70 monoclonal antibody (SPA-810) and Hsp90 monoclonal antibody (SPA-830) were purchased from Stressgen (Victoria, Canada). Anti-αB-crystallin antibody was purchased from Calbiochem (238702). Secondary antibodies conjugated to rhodamine (RRX), Cy5 or HRP were from Jackson ImmunoResearch (West Grove, PA).

Protein analysis and proteasomal activity assay

Cells were lysed in cold Triton-DOC lysis buffer (0.5% TX-100, 0.25% Na-deoxycholate, 150 mM NaCl, 10 mM Tris-Cl pH 7.5, 10 mM EDTA). The lysates were spun for 3 minutes at 5000 rpm (2350 ***g***) in a desktop microfuge. Biochemical analyses were performed on the post-nuclear supernatant (PNS). Proteins were transferred to PVDF membrane and blots were developed using an ECL system. In vitro proteasome activity assays were performed using Z-GGL-AMC, according to the manufacturer's instructions.

Immunofluorescent microscopy and live imaging

To detect PrP, cells were grown on poly-D-lysine-coated chamber slides (Nunc, #155411), fixed (10% formalin in PBS, 30 minutes, RT), quenched with cold 1% NH_4Cl in PBS, permeabilized (0.1% TX-100 in PBS, 2 minutes, RT) and blocked with 2% BSA (30 minutes, RT). The cells were then incubated with the primary anti-PrP antibody (in 1% BSA, overnight, 4°C), rinsed and the secondary anti-PrP antibody conjugated to rhodamine (diluted 1:300 in 1% BSA) was added for 30 minutes (RT). The labeled cells were mounted in an anti-fading preparation (5% *n*-propyl gallate, 100 mM Tris-Cl pH 9, 70% glycerol) and viewed with a Zeiss axiovert 135 confocal microscope.

For time-lapse microscopy, FRAP and FLIP experiments, cells were plated on poly-L-lysine (Sigma) coated glass-bottom plates (MatTek Corp, #P35GC-1.0-14-C) or on a chambered coverglass system (Nunc, #177445). Confocal microscopy was conducted using a Zeiss LSM 710 Axio Observer.Z1 laser scanning microscope with a 63× oil for FRAP, FLIP and immunofluorescence, and an LD Plan-Neofluar 40×/0.6 Corr M27 objective for time-lapse microscopy, in an XL LSM 710 S1 incubator at 37°C and 5% CO_2. For time-lapse experiments, Z-stack series of 1 um scans were collected in 10 minute intervals for 16 hours. For FRAP, a region of interest was bleached using a 488 nm laser for 2 seconds at full laser power and single scan images were collected every 1 second for 1 minute following the bleach. Fluorescence of the bleached region of interest (F) was calculated as F=(Ii–Ib)/(Ir–Ib), where Ii is fluorescence intensity in the region of interest, Ir is intensity in a reference area (either at some distance in the same cell or in another cell) and Ib is background intensity (outside all cells). Intensity data were recorded using Zeiss ZEN software. Reported values are the average of at least three data points. Zeiss ZEN and ImageJ software was used for processing and quantification. For FLIP experiments, a 2×2 µm area of the cytosol was bleached continuously (with each scan), while the fluorescence of the inclusion and a control cytosolic region close to the inclusion was measured.

Modified FPP assay

YFP–PrP or naïve CHO cells were seeded on 35 mm cover glass MatTek plates. 24 hours later, naïve cells were transfected with either HttQ97–RFP or ChFP–VHL. CHO-YFP–PrP cells were treated with 60 µg/ml CsA for 18 hours. Prior to imaging, cells were washed three times in KHM buffer (110 mM potassium acetate, 20 mM HEPES, 2 mM $MgCl_2$). JUNQ, IPOD or YFP–PrP inclusions were located and first images recorded for pre-permeabilization images. Digitonin in KHM buffer was added to a final concentration of 120 µM (a concentration determined experimentally as appropriate for selective permeabilization of the plasma membrane). 500 mM trypsin or 50 µg/ml PK (in KHM buffer) was added after cytosolic permeabilization (140 seconds in these cells). Throughout the time course, images were captured at 1 second intervals (Lorenz et al., 2006) (S. J. Weisberg et al., unpublished).

HPLC

In order to test for CsA removal, fifteen 10 cm plates of CHO-YFP–PrP cells were incubated with 60 µg/ml CsA or with ethanol for 16 hours, then rinsed and incubated in fresh media for an additional 16 hours before harvest. Positive control plates were supplemented with 60 µg/ml CsA 16 hours prior to harvest. Cells were rinsed three times with ice-cold PBS, scraped and centrifuged. Pellets were resuspended in ethyl acetate (3 ml for 150 µl). Samples were vortexed for 5 minutes, and 2.8 ml of the organic phase was transferred and vacuum dried. 120 µl of the running phase was added and the samples were analyzed by HPLC. A computer-controlled Waters chromatograph with the following components was used: Millennium software (version 3.2), 600E multisolvent delivery pump, 20 µl loop and photodiode array (996-model) detector. All solvents were HPLC grade; acetonitrile and methanol were from J. T. Baker (Deventer, Holland). Water was deionized, doubly distilled and filtered through 0.2 µm cellulose mixed ester membrane (Schleicher & Schuell). All solvent reservoirs were purged with helium at 100 ml/minute flow for 30 minutes before the run and at 30 ml/minute during the run. Crude samples were filtered before injection by loading concentrated portions of extracts onto 0.2 µm nylon syringe filters and analysis performed on an analytical column of Waters Symmetry C18 (5 µM, 4.6×250 mm). A 30 µl aliquot was injected and analyzed by gradient reversed-phase mode at room temperature (25°C). Running phase at the beginning of the run was composed of 30% water, 50% acetonitrile and 20% methanol, at a flow of 1 ml/minute. 1 minute into running, the composition began to gradually change, reaching 100% acetonitrile at 10 minutes. Between 20 and 25 minutes, the running phase returned gradually to the original composition, after which composition was maintained for 25 more minutes, a total of 55 minutes per run.

This study was generously supported by the Rosalinde and Arthur Gilbert Foundation (AFAR) and the Levi Foundation. T.B.-G. is supported by the Anonymous and the Lady Davis Foundations. This research project was also supported in part by a grant from the USAID American Schools and Hospitals Abroad (ASHA) program for the procurement of confocal microscope LSM710. E.C. and T.B.-G. initiated and designed this study, and wrote the manuscript. T.B.-G. performed western blotting, immunofluorescence, live imaging, FPP, FRAP and FLIP experiments. R.L. performed immunofluoresence experiments, N.M.K. carried out HPLC, M.V.K. created the YFP–PrP plasmid, M.B.-S. performed western blotting, D.K. performed FRAP and FLIP experiments, D.K. and Y.Y. helped write the manuscript.

Supplementary material available online at
http://jcs.biologists.org/cgi/content/full/124/11/1891/DC1

References

Aguzzi, A. and Calella, A. M. (2009). Prions: protein aggregation and infectious diseases. *Physiol. Rev.* **89**, 1105-1152.

Bagola, K. and Sommer, T. (2008). Protein quality control: on IPODs and other JUNQ. *Curr. Biol.* **18**, R1019-R1021.

Balch, W. E., Morimoto, R. I., Dillin, A. and Kelly, J. W. (2008). Adapting proteostasis for disease intervention. *Science* **319**, 916-919.

Barik, S. (2006). Immunophilins: for the love of proteins. *Cell. Mol. Life Sci.* **63**, 2889-2900.

Bates, G. (2003). Huntingtin aggregation and toxicity in Huntington's disease. *Lancet* **361**, 1642-1644.

Behrends, C., Langer, C. A., Boteva, R., Bottcher, U. M., Stemp, M. J., Schaffar, G., Rao, B. V., Giese, A., Kretzschmar, H., Siegers, K. et al. (2006). Chaperonin TRiC promotes the assembly of polyQ expansion proteins into nontoxic oligomers. *Mol. Cell* **23**, 887-897.

Bercovich, Z., Rosenberg-Hasson, Y., Ciechanover, A. and Kahana, C. (1989). Degradation of ornithine decarboxylase in reticulocyte lysate is ATP-dependent but ubiquitin-independent. *J. Biol. Chem.* **264**, 15949-15952.

Bieschke, J., Cohen, E., Murray, A., Dillin, A. and Kelly, J. W. (2009). A kinetic assessment of the C. elegans amyloid disaggregation activity enables uncoupling of disassembly and proteolysis. *Protein Sci.* **18**, 2231-2241.

Ciechanover, A. and Brundin, P. (2003). The ubiquitin proteasome system in neurodegenerative diseases: sometimes the chicken, sometimes the egg. *Neuron* **40**, 427-446.

Cohen, E. and Taraboulos, A. (2003). Scrapie-like prion protein accumulates in aggresomes of cyclosporin A-treated cells. *EMBO J.* **22**, 404-417.

Cohen, E., Bieschke, J., Perciavalle, R. M., Kelly, J. W. and Dillin, A. (2006). Opposing activities protect against age-onset proteotoxicity. *Science* **313**, 1604-1610.

Cohen, E., Paulsson, J. F., Blinder, P., Burstyn-Cohen, T., Du, D., Estepa, G., Adame, A., Pham, H. M., Holzenberger, M., Kelly, J. W. et al. (2009). Reduced IGF-1 signaling delays age-associated proteotoxicity in mice. *Cell* **139**, 1157-1169.

Cummings, C. J., Sun, Y., Opal, P., Antalffy, B., Mestril, R., Orr, H. T., Dillmann, W. H. and Zoghbi, H. Y. (2001). Over-expression of inducible HSP70 chaperone suppresses neuropathology and improves motor function in SCA1 mice. *Hum. Mol. Genet.* **10**, 1511-1518.

Dantuma, N. P., Lindsten, K., Glas, R., Jellne, M. and Masucci, M. G. (2000). Short-lived green fluorescent proteins for quantifying ubiquitin/proteasome-dependent proteolysis in living cells. *Nat. Biotechnol.* **18**, 538-543.

Falsone, S. F., Kungl, A. J., Rek, A., Cappai, R. and Zangger, K. (2009). The molecular chaperone Hsp90 modulates intermediate steps of amyloid assembly of the Parkinson-related protein alpha-synuclein. *J. Biol. Chem.* **284**, 31190-31199.

Freude, S., Hettich, M. M., Schumann, C., Stohr, O., Koch, L., Kohler, C., Udelhoven, M., Leeser, U., Muller, M., Kubota, N. et al. (2009). Neuronal IGF-1 resistance reduces Abeta accumulation and protects against premature death in a model of Alzheimer's disease. *FASEB J.* **23**, 3315-3324.

Garcia-Mata, R., Bebok, Z., Sorscher, E. J. and Sztul, E. S. (1999). Characterization and dynamics of aggresome formation by a cytosolic GFP-chimera. *J. Cell Biol.* **146**, 1239-1254.

Hartl, F. U. and Hayer-Hartl, M. (2002). Molecular chaperones in the cytosol: from nascent chain to folded protein. *Science* **295**, 1852-1858.

Hartl, F. U. and Hayer-Hartl, M. (2009). Converging concepts of protein folding in vitro and in vivo. *Nat. Struct. Mol. Biol.* **16**, 574-581.

Hirsch, C., Gauss, R., Horn, S. C., Neuber, O. and Sommer, T. (2009). The ubiquitylation machinery of the endoplasmic reticulum. *Nature* **458**, 453-460.

Hsiao, K., Baker, H. F., Crow, T. J., Poulter, M., Owen, F., Terwilliger, J. D., Westaway, D., Ott, J. and Prusiner, S. B. (1989). Linkage of a prion protein missense variant to Gerstmann-Straussler syndrome. *Nature* **338**, 342-345.

Johnston, J. A., Ward, C. L. and Kopito, R. R. (1998). Aggresomes: a cellular response to misfolded proteins. *J. Cell Biol.* **143**, 1883-1898.

Kaganovich, D., Kopito, R. and Frydman, J. (2008). Misfolded proteins partition between two distinct quality control compartments. *Nature* **454**, 1088-1095.

Kawaguchi, Y., Kovacs, J. J., McLaurin, A., Vance, J. M., Ito, A. and Yao, T. P. (2003). The deacetylase HDAC6 regulates aggresome formation and cell viability in response to misfolded protein stress. *Cell* **115**, 727-738.

Kim, S., Nollen, E. A., Kitagawa, K., Bindokas, V. P. and Morimoto, R. I. (2002). Polyglutamine protein aggregates are dynamic. *Nat. Cell Biol.* **4**, 826-831.
Kopito, R. R. and Ron, D. (2000). Conformational disease. *Nat. Cell Biol.* **2**, E207-E209.
Kristiansen, M., Messenger, M. J., Klohn, P. C., Brandner, S., Wadsworth, J. D., Collinge, J. and Tabrizi, S. J. (2005). Disease-related prion protein forms aggresomes in neuronal cells leading to caspase activation and apoptosis. *J. Biol. Chem.* **280**, 38851-38861.
Kristiansen, M., Deriziotis, P., Dimcheff, D. E., Jackson, G. S., Ovaa, H., Naumann, H., Clarke, A. R., van Leeuwen, F. W., Menendez-Benito, V., Dantuma, N. P. et al. (2007). Disease-associated prion protein oligomers inhibit the 26S proteasome. *Mol. Cell* **26**, 175-188.
Liberek, K., Lewandowska, A. and Zietkiewicz, S. (2008). Chaperones in control of protein disaggregation. *EMBO J.* **27**, 328-335.
Lippincott-Schwartz, J., Altan-Bonnet, N. and Patterson, G. H. (2003). Photobleaching and photoactivation: following protein dynamics in living cells. *Nat. Cell Biol.* **Suppl**, S7-S14.
Lorenz, H., Hailey, D. W., Wunder, C. and Lippincott-Schwartz, J. (2006). The fluorescence protease protection (FPP) assay to determine protein localization and membrane topology. *Nat. Protoc.* **1**, 276-279.
Ma, J. and Lindquist, S. (2001). Wild-type PrP and a mutant associated with prion disease are subject to retrograde transport and proteasome degradation. *Proc. Natl. Acad. Sci. USA* **98**, 14955-14960.
Mishra, R. S., Bose, S., Gu, Y., Li, R. and Singh, N. (2003). Aggresome formation by mutant prion proteins: the unfolding role of proteasomes in familial prion disorders. *J. Alzheimers Dis.* **5**, 15-23.
Muchowski, P. J. and Wacker, J. L. (2005). Modulation of neurodegeneration by molecular chaperones. *Nat. Rev. Neurosci.* **6**, 11-22.
Muchowski, P. J., Schaffar, G., Sittler, A., Wanker, E. E., Hayer-Hartl, M. K. and Hartl, F. U. (2000). Hsp70 and Hsp40 chaperones can inhibit self-assembly of polyglutamine proteins into amyloid-like fibrils. *Proc. Natl. Acad. Sci. USA* **97**, 7841-7846.
Muchowski, P. J., Ramsden, R., Nguyen, Q., Arnett, E. E., Greiling, T. M., Anderson, S. K. and Clark, J. I. (2008). Noninvasive measurement of protein aggregation by mutant huntingtin fragments or alpha-synuclein in the lens. *J. Biol. Chem.* **283**, 6330-6336.
Outeiro, T. F., Klucken, J., Strathearn, K. E., Liu, F., Nguyen, P., Rochet, J. C., Hyman, B. T. and McLean, P. J. (2006). Small heat shock proteins protect against alpha-synuclein-induced toxicity and aggregation. *Biochem. Biophys. Res. Commun.* **351**, 631-638.
Peretz, D., Williamson, R. A., Legname, G., Matsunaga, Y., Vergara, J., Burton, D. R., DeArmond, S. J., Prusiner, S. B. and Scott, M. R. (2002). A change in the conformation of prions accompanies the emergence of a new prion strain. *Neuron* **34**, 921-932.
Rosenberg-Hasson, Y., Bercovich, Z., Ciechanover, A. and Kahana, C. (1989). Degradation of ornithine decarboxylase in mammalian cells is ATP dependent but ubiquitin independent. *Eur. J. Biochem.* **185**, 469-474.
Schonbrunner, E. R., Mayer, S., Tropschug, M., Fischer, G., Takahashi, N. and Schmid, F. X. (1991). Catalysis of protein folding by cyclophilins from different species. *J. Biol. Chem.* **266**, 3630-3635.
Scott, M. R., Kohler, R., Foster, D. and Prusiner, S. B. (1992). Chimeric prion protein expression in cultured cells and transgenic mice. *Protein Sci.* **1**, 986-997.
Selkoe, D. J. (2003). Folding proteins in fatal ways. *Nature* **426**, 900-904.
Serban, D., Taraboulos, A., DeArmond, S. J. and Prusiner, S. B. (1990). Rapid detection of Creutzfeldt-Jakob disease and scrapie prion proteins. *Neurology* **40**, 110-117.
Shorter, J. and Lindquist, S. (2004). Hsp104 catalyzes formation and elimination of self-replicating Sup35 prion conformers. *Science* **304**, 1793-1797.
Silveira, J. R., Raymond, G. J., Hughson, A. G., Race, R. E., Sim, V. L., Hayes, S. F. and Caughey, B. (2005). The most infectious prion protein particles. *Nature* **437**, 257-261.
Stewart, D. P., Koss, B., Bathina, M., Perciavalle, R. M., Bisanz, K. and Opferman, J. T. (2010). Ubiquitin-independent degradation of antiapoptotic MCL-1. *Mol. Cell. Biol.* **30**, 3099-3110.
Tofaris, G. K., Layfield, R. and Spillantini, M. G. (2001). alpha-synuclein metabolism and aggregation is linked to ubiquitin-independent degradation by the proteasome. *FEBS Lett.* **509**, 22-26.
Tyedmers, J., Treusch, S., Dong, J., McCaffery, J. M., Bevis, B. and Lindquist, S. (2010). Prion induction involves an ancient system for the sequestration of aggregated proteins and heritable changes in prion fragmentation. *Proc. Natl. Acad. Sci. USA* **107**, 8633-8638.
Yamazaki, M., Oyanagi, K., Mori, O., Kitamura, S., Ohyama, M., Terashi, A., Kitamoto, T. and Katayama, Y. (1999). Variant Gerstmann-Straussler syndrome with the P105L prion gene mutation: an unusual case with nigral degeneration and widespread neurofibrillary tangles. *Acta Neuropathol.* **98**, 506-511.
Yedidia, Y., Horonchik, L., Tzaban, S., Yanai, A. and Taraboulos, A. (2001). Proteasomes and ubiquitin are involved in the turnover of the wild-type prion protein. *EMBO J.* **20**, 5383-5391.